



Cite this: DOI: 10.1039/d5va00433k

# Spatial and temporal variations of ambient PM<sub>2.5</sub>, NO<sub>2</sub>, and O<sub>3</sub> in Kigali: evidence and policy implications from a multi-year, citywide monitoring network

Augustine Omodieke, Daniel Twum and Egide Kalisa \*

Air pollution is increasingly concerning for the environment and health in Africa, yet high-resolution, dependable data are limited. This study provides a comprehensive assessment of air quality in Kigali city, Rwanda's capital, using real-time PM<sub>2.5</sub>, NO<sub>2</sub>, and O<sub>3</sub> measurements from 11 stations across three districts (Gasabo, Kicukiro, and Nyarugenge) spanning 2021 to 2024. All data were collected using a low-cost sensor (Real-time Affordable Multi-Pollutant (RAMP)) and validated with data from a reference-grade Beta Attenuation Mass Monitor (BAM). The results show that PM<sub>2.5</sub> levels regularly exceed WHO guidelines across all seasons, with annual averages ranging from 33.6 to 46.3  $\mu\text{g m}^{-3}$  and peak episodes exceeding 200  $\mu\text{g m}^{-3}$ , especially during dry months. NO<sub>2</sub> levels ranged from 18.6 to 22.9  $\mu\text{g m}^{-3}$  annually, with the peak hourly concentration reaching 173  $\mu\text{g m}^{-3}$  at roadside locations. O<sub>3</sub> displayed significant seasonal changes, with 8 hour maximums reaching nearly 58 ppb. PM<sub>2.5</sub> and O<sub>3</sub> concentrations at the urban roadside sites were significantly higher than those at the urban background and rural sites. This is the first comprehensive long-term citywide air quality study in Rwanda, providing an essential baseline for informed policymaking and regional comparisons across sub-Saharan Africa. Our findings highlight the need to expand the deployment of low-cost sensor networks in vulnerable urban neighbourhoods to understand local-scale air pollution episodes and rapidly inform local interventions.

Received 24th November 2025  
Accepted 20th March 2026

DOI: 10.1039/d5va00433k

rsc.li/esadvances

## Environmental significance

Air pollution remains a significant yet under-monitored threat in sub-Saharan Africa. Due to limited capacity and the high cost of reference monitoring equipment, data on the spatial and seasonal patterns of pollutants are scarce. This study presents the first multi-season evaluation of ambient air quality in Rwanda, utilizing validated, low-cost sensor networks. The findings reveal persistent exceedances of the WHO particulate matter and Ozone thresholds in urban areas, highlighting health risks in rapidly growing African cities. By demonstrating the effectiveness of scalable air monitoring tools, this research supports region-specific policies, raises community awareness, and advances environmental justice. It provides an evidence base for low-resource governments seeking cost-effective strategies to track and mitigate urban air pollution.

## 1 Introduction

Air pollution is a leading global environmental health threat, responsible for an estimated 7 million premature deaths each year.<sup>1</sup> Fine particulate matter (PM<sub>2.5</sub>), nitrogen dioxide (NO<sub>2</sub>), and ozone (O<sub>3</sub>) are among the most critical urban air pollutants, associated with respiratory and cardiovascular morbidity and mortality, particularly in vulnerable populations.<sup>1,2</sup> In 2021, the World Health Organization (WHO) tightened its air quality guidelines, significantly lowering acceptable thresholds for these pollutants.<sup>3</sup> However, air pollution in rapidly industrializing and developing regions remains at catastrophic levels,

posing significant health concerns.<sup>4,5</sup> Cities across Africa, Asia, and Latin America routinely experience annual PM<sub>2.5</sub> concentrations that are multiple times higher than the WHO-recommended level of 5  $\mu\text{g m}^{-3}$ .<sup>6,7</sup> Likewise, daily NO<sub>2</sub> and O<sub>3</sub> concentrations often exceed the limits set to protect public health. These pollutants also contribute to environmental degradation, reduced crop yields, and climate change, with ozone acting as a short-lived climate pollutant.<sup>8</sup> Although the global overview remains concerning, air quality varies widely by region.<sup>9</sup> Many high-income countries in Europe and North America have achieved cleaner air in recent decades through deliberate, stringent policies and actions, including reductions in industrial emissions and technological advancements that have led to a shift toward energy-efficient vehicles.<sup>10-13</sup>

Across Africa, air quality varies widely due to differences in emission sources and climatic conditions.<sup>14,15</sup> In North Africa,

Department of Epidemiology and Biostatistics, Schulich School of Medicine and Dentistry, Western University, London, Ontario, N6G 2M1, Canada. E-mail: ekalisa2@uwo.ca



countries like Egypt and Algeria face high levels of particulate pollution from desert dust, compounded by urban emissions.<sup>16</sup> West African coastal cities, including Lagos, Accra, and Abidjan, contend with traffic congestion, diesel generators, and open waste burning.<sup>17,18</sup> Central Africa experiences episodic pollution spikes from biomass burning, while Southern Africa's persistent particulate matter emissions stem from heavy industry and mining.<sup>19</sup> In East Africa, pollution is influenced by urban growth, traffic emissions, and traditional cooking practices.<sup>20,21</sup> Kigali, Rwanda's capital, exemplifies this complexity, with significant intra-urban differences in pollutant levels. For example, roadside and commercial zones exhibit elevated levels of NO<sub>2</sub> and PM<sub>2.5</sub> due to vehicle emissions and resuspended dust.<sup>22</sup> In Accra, NO<sub>2</sub> levels were as high as 76 µg m<sup>-3</sup> in traffic-heavy areas, compared with 24 µg m<sup>-3</sup> in peri-urban areas.<sup>23</sup> In Kigali, wood- and charcoal-cooking in peri-urban areas increases PM<sub>2.5</sub> levels, especially in the evening.<sup>24</sup> Seasonal dryness amplifies these effects, with ozone peaking up to 70 ppb in Rwanda's dry season.<sup>25</sup>

In sub-Saharan African countries such as Rwanda, significant data and research gaps remain in understanding urban air pollution.<sup>26–28</sup> Most cities lack long-term, high-resolution monitoring networks and instead rely on short-term field campaigns, low-cost sensors, or satellite estimates.<sup>29,30</sup> These methods, while helpful, often lack the detail needed for effective policy action. Monitoring infrastructure is sparse and underfunded, with limited coverage beyond a few countries. Epidemiological studies linking pollution to health outcomes are almost non-existent, making it difficult to assess local health risks.<sup>31–33</sup> Although PM<sub>2.5</sub> monitoring is expanding, there is still a critical gap in data on NO<sub>2</sub> and O<sub>3</sub>, both key pollutants.<sup>29</sup>

Kigali, Rwanda's capital, is pursuing ambitious environmental goals through its “Green City” initiative and emerging air-quality management policies.<sup>34</sup> However, data on ambient air quality remain limited and fragmented, with few studies providing long-term, multi-pollutant monitoring across diverse site types. Rapid urbanization, population growth, and increasing vehicle ownership have intensified pollution sources over the past decade.<sup>26,35</sup> Kigali's complex topography of valleys and ridges<sup>22</sup> further exacerbates air stagnation, trapping pollutants during temperature inversions. The city's tropical climate, characterized by two dry and two wet seasons, strongly influences pollutant dispersion and chemical transformation. Combined emissions from vehicles, biomass burning, and open waste incineration create spatially and temporally variable pollution patterns.<sup>36</sup> These characteristics make Kigali an ideal case for examining urban air pollution dynamics in a rapidly developing African context, where emissions remain relatively low but increasing, and where evidence-based monitoring is essential for guiding emerging environmental and public health policies.<sup>21,29</sup>

To begin addressing these gaps, this study presents a comprehensive, multi-year assessment of ambient PM<sub>2.5</sub>, NO<sub>2</sub>, and O<sub>3</sub> levels in Kigali, Rwanda, using a dense network of fixed monitoring stations spanning urban background, roadside, and rural locations across the city's three districts. The objectives of

this study are three-fold: (i) to quantify the spatial and seasonal variability of PM<sub>2.5</sub>, NO<sub>2</sub>, and O<sub>3</sub> across Kigali; (ii) to characterize diurnal patterns and pollutant interactions; and (iii) to provide an evidence base to support urban air quality management and policy formulation in Rwanda and similar settings. By bridging empirical gaps and offering policy-relevant insights,<sup>37</sup> this research contributes to both the scientific and practical advancement of air quality governance in Africa.

## 2 Methods and materials

### 2.1 Study area

Rwanda is a landlocked nation in East Africa's Great Lakes region, covering about 26 338 km<sup>2</sup> and characterized by hills. As of 2023, it has one of Africa's highest population densities, at 566 people per square kilometre.<sup>38</sup> The country has a tropical highland climate shaped by its elevation, with average temperatures between 16 °C and 20 °C.<sup>36</sup> Rwanda experiences two main seasons: a long rainy season from March to May and a shorter rainy season from October to December, separated by two dry seasons from June to September and from December to February.<sup>36</sup> This study examines Kigali City (Fig. 1), the capital and economic center of Rwanda, located at 1.95°S and 30.09°E, at an altitude of approximately 1567 meters. The city is split into three districts, including Gasabo, Kicukiro, and Nyarugenge, each with unique urban, social, and environmental features. Gasabo, the largest, includes peri-urban and semi-rural zones with a mix of residential and farming lands. Kicukiro is primarily a suburban region that is developing rapidly in its industrial and commercial sectors. Meanwhile, Nyarugenge functions as the historic and commercial center of the city, characterized by its high population density, regular traffic congestion, and a focus of economic activities.

Air quality was evaluated across the three districts using 11 strategically located monitoring stations to detect spatial variations in pollution levels. The data, collected from May 2021 to

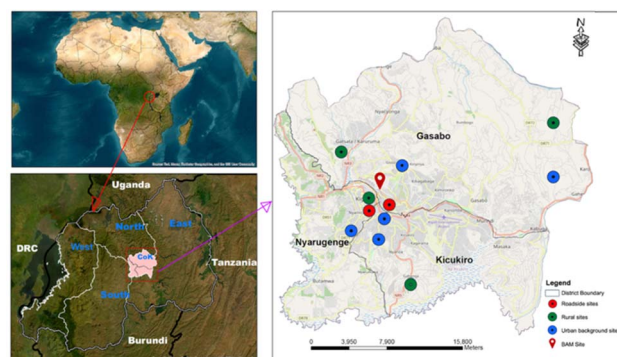


Fig. 1 Map of Africa showing the geographic location of Rwanda, the city of Kigali, and the three districts of Gasabo, Kicukiro and Nyarugenge. Source: The satellite imagery was obtained using ArcGIS Desktop version 10.8 (Esri, Redlands, CA, USA) with the default “World Imagery” basemaps provided through ArcGIS Online. The imagery is sourced from ESRI, DigitalGlobal, GeoEye, and Earthstar Geographics, and is used in accordance with ESRI's terms of use for publications. <https://www.esri.com/en-us/arcgis/products/arcgis-desktop/overview>.



December 2024, comprises hourly measurements of  $\text{PM}_{2.5}$ ,  $\text{NO}_2$ , and  $\text{O}_3$ , which are crucial air pollution indicators in swiftly growing African cities.

## 2.2 Sampling and instrumentation

Real-time air quality measurements of  $\text{PM}_{2.5}$ ,  $\text{NO}_2$ , and  $\text{O}_3$  were collected between May 2021 and December 2024 across 11 monitoring sites in Kigali City (Fig. 1) using low-cost Real-time Affordable Multi-Pollutant (RAMP) monitors (SENSIT Technologies, USA). Each RAMP unit was mounted 2–3 m above ground level and equipped with Alphasense electrochemical sensors (UK) for gas ( $\text{NO}_2$  and  $\text{O}_3$ ) measurements and a particle sensor for  $\text{PM}_{2.5}$ . The instruments simultaneously recorded meteorological parameters, including temperature and relative humidity. Sensor signals were processed and averaged to yield 60 second measurements. Calibration and performance of the low-cost gas sensors used in this study were established following previous works,<sup>39,40</sup> and detailed in our previous study.<sup>22</sup> Hourly concentrations were derived using generalized RAMP (gRAMP) calibration models developed from extended collocations with reference-grade instruments in Pittsburgh, USA. For  $\text{O}_3$ , a hybrid random forest-linear regression model was applied. Mean Absolute Error (MAEs) of  $\sim 3.5$  ppb and  $\sim 3.4$  ppb were reported for  $\text{NO}_2$  and  $\text{O}_3$ , respectively, with Pearson  $r$  values typically  $>0.8$ , aligning with US EPA Air Sensor Guidebook benchmarks for exposure assessment. For local data validation of our study,  $\text{PM}_{2.5}$  measurements from the RAMP sensors were compared against co-located reference data from the Beta Attenuation Mass Monitor (BAM) operated by the U.S. Embassy in Kigali (<https://www.airnow.gov/>). The BAM station, situated about 5–10 km from the study sites, functions as the city's reference point for air quality monitoring. Correlations were statistically significant ( $r = 0.96$ ,  $p < 0.001$ ), indicating a very strong linear agreement between our RAMPs and reference-grade BAM and underscores the reliability of the low-cost sensors used in this study. Due to limitations in data access, we did not perform local verification of  $\text{NO}_2$  and  $\text{O}_3$  levels in this study. Nonetheless, prior evaluations employed rigorous quality control using generalized RAMP (gRAMP) calibration models,<sup>36</sup> which our study relied on, including a local validation of  $\text{O}_3$  performance conducted at the Rwanda Climate Observatory through a short-term collocation with reference analyzers, demonstrating comparable model performance under regional conditions.<sup>41</sup>

## 2.3 Data quality assurance

To ensure data quality and assess measurement accuracy, we compared district-level  $\text{PM}_{2.5}$  measurements with collocated reference-grade values from a Beta Attenuation Mass Monitor (BAM). Correlation analysis was conducted using the 2023 dataset across all three districts of Gasabo, Kicukiro, and Nyarugenge, which represented the only full year of complete and continuous overlap between the BAM reference monitor and all RAMP units. Correlations were statistically significant at both temporal scales. At the hourly level,  $r = 0.66$  ( $p < 0.001$ ), while at the monthly level the correlation strengthened substantially ( $r = 0.96$ ,  $p < 0.001$ ) (Fig. 2). This indicates a very strong linear agreement between our RAMPs and reference-

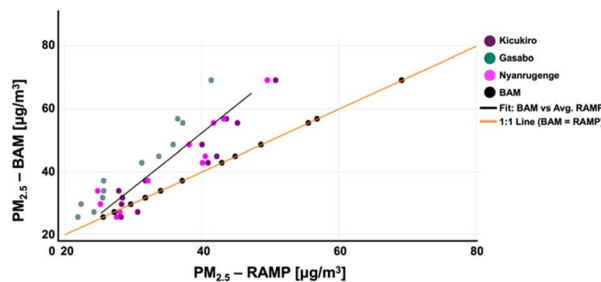


Fig. 2 Comparison of mean  $\text{PM}_{2.5}$  measurements from Kigali districts' Real-time Affordable Multi-Pollutant (RAMP) monitors against Beta Attenuation Monitor (BAM) reference instrument in Kicukiro, Gasabo, and Nyarugenge districts for the year 2023. The panel displays a scatter plot of monthly-averaged  $\text{PM}_{2.5}$  concentrations, with Pearson correlation coefficient ( $r = 0.96$ ) and  $p$ -value ( $<0.001$ ), demonstrating a statistically significant linear relationship. The fitted line represents a linear regression of BAM  $\text{PM}_{2.5}$  on RAMP  $\text{PM}_{2.5}$ .

grade BAM and underscores the reliability of the low-cost sensors used in this study. The stronger correlation observed at the monthly scale ( $r = 0.96$ ) compared with the hourly scale ( $r = 0.66$ ) reflects the influence of short-term spatial heterogeneity and meteorological variability, which introduce noise at finer temporal resolution. Temporal averaging reduces this variability and strengthens agreement between instruments.

Across the study period, RAMP  $\text{PM}_{2.5}$  measurements were generally lower than BAM observations, indicating a systematic underestimation by the low-cost sensors. This bias is evident from the clustering of points above the 1 : 1 line (BAM = RAMP), consistent with BAM concentrations exceeding corresponding RAMP values. The data spread likely reflects site-level differences in microenvironments, meteorological conditions, and sensor calibration drift, all of which influence how RAMP monitors track  $\text{PM}_{2.5}$  relative to the BAM reference. However, the strong, statistically significant linear correlation between BAM and RAMP values suggests that, despite the bias, RAMP sensors effectively track temporal variability in pollution levels. They remain a valuable tool for spatially distributed, real-time air quality monitoring, especially in resource-constrained urban settings like Kigali.

## 2.4 Statistical analyses

Descriptive summaries were generated for all variables, and their distributions were visually inspected using histograms and quantile–quantile (Q–Q) plots. Given that particulate matter ( $\text{PM}_{2.5}$ ), ozone ( $\text{O}_3$ ), nitrogen dioxide ( $\text{NO}_2$ ) and temperature data were not normally distributed, nonparametric methods were employed. Specifically, the Kruskal–Wallis test was used to compare differences in means across the different microenvironments for these variables. In contrast, relative humidity (RH) data followed an approximately normal distribution, and one-way ANOVA was used for RH comparisons. To evaluate the relationship between BAM and RAMP  $\text{PM}_{2.5}$  measurements, linear regression was performed, and the statistical significance of the correlation was determined using a  $t$ -test on the slope of the fitted regression line. All statistical



tests were two-sided, and results were considered statistically significant at a  $p$ -value threshold of  $<0.05$ . All statistical analyses were conducted using R (version 4.3.2) and Stata 14 (SE 14.2).

### 3 Results

#### 3.1 Spatial distribution of pollutants by district

Our assessment of PM<sub>2.5</sub>, NO<sub>2</sub>, and O<sub>3</sub> levels across Gasabo, Kicukiro, and Nyarugenge districts in Kigali revealed significant spatial variations. The data in Table 1 indicate notable differences in pollutant concentrations and meteorological conditions across these districts, providing essential insights for assessing local exposure risks and shaping policy development.

Mean PM<sub>2.5</sub> concentrations varied significantly across districts ( $p < 0.001$ ). Nyarugenge recorded the highest mean level ( $45.8 \pm 27.6 \mu\text{g m}^{-3}$ ), followed by Kicukiro ( $41.5 \pm 16.2 \mu\text{g m}^{-3}$ ), and Gasabo ( $37.9 \pm 17.5 \mu\text{g m}^{-3}$ ). NO<sub>2</sub> concentrations also differed significantly ( $p < 0.001$ ), with Nyarugenge ( $22.9 \pm 6.5 \mu\text{g m}^{-3}$ ) and Gasabo ( $21.2 \pm 6.5 \mu\text{g m}^{-3}$ ) showing higher levels than Kicukiro ( $15.2 \pm 4.2 \mu\text{g m}^{-3}$ ). O<sub>3</sub> concentrations ranged from  $18.9 \pm 6.6$  ppb in Gasabo to  $25.5 \pm 18.4$  ppb in Nyarugenge ( $p < 0.001$ ). The elevated PM<sub>2.5</sub>, NO<sub>2</sub>, and O<sub>3</sub> concentrations observed in Nyarugenge likely reflect its higher urban density, traffic intensity, and commercial activity, which increase primary emissions and promote secondary pollutant formation. In contrast, lower levels in Gasabo may be partly attributable to greater residential dispersion, vegetation cover, and enhanced pollutant dilution. Meteorological data showed small but significant differences in mean temperature and relative humidity across districts.

#### 3.2 Spatial distribution of pollutants by land-use type

Our pollutant measurements across different microenvironments in Kigali's roadside, rural, and urban background sites

showed clear differences in levels of particulate matter, nitrogen dioxide, and ozone. Additionally, meteorological conditions varied, influencing exposure risks in these areas. PM<sub>2.5</sub> concentrations varied markedly and statistically significantly across microenvironments ( $p < 0.001$ ). Roadside sites recorded the highest mean annual level ( $52.2 \mu\text{g m}^{-3}$ ), followed by urban background locations ( $42.3 \mu\text{g m}^{-3}$ ) and rural areas ( $37.5 \mu\text{g m}^{-3}$ ) (Table 1). The peak concentration reached  $249 \mu\text{g m}^{-3}$  at a roadside site, underscoring severe episodic pollution along traffic corridors. NO<sub>2</sub> concentrations also differed significantly ( $p < 0.001$ ), with the highest mean value observed in rural areas ( $21.4 \mu\text{g m}^{-3}$ ), followed by urban background sites ( $20.6 \mu\text{g m}^{-3}$ ) and roadside locations ( $19.3 \mu\text{g m}^{-3}$ ). O<sub>3</sub> concentrations displayed a gradient across microenvironments ( $p < 0.001$ ), ranging from 19.4 ppb at urban background sites to 21.1 ppb in rural areas and peaking at 28.3 ppb along roadsides. The pronounced PM<sub>2.5</sub> and O<sub>3</sub> enhancements at roadside sites highlight the combined effects of traffic emissions, resuspended dust, and localized photochemical production. Higher NO<sub>2</sub> levels at rural and urban background sites may reflect pollutant aging, reduced dispersion, and contributions from domestic combustion, illustrating how microenvironmental conditions shape exposure beyond simple proximity to traffic. Meteorological parameters also showed statistically significant differences, with the highest mean ambient temperature recorded at urban background sites ( $21.8 \text{ }^\circ\text{C}$ ), followed by roadside ( $20.7 \text{ }^\circ\text{C}$ ) and rural areas ( $20.2 \text{ }^\circ\text{C}$ ).

#### 3.3 Monthly patterns in mean PM<sub>2.5</sub>, NO<sub>2</sub>, and O<sub>3</sub> levels across land-use types

Fig. 3 shows how the levels of PM<sub>2.5</sub>, NO<sub>2</sub>, and O<sub>3</sub> change with the seasons across three different site types in Kigali, including roadside, rural, and urban background from 2021 to 2024.

Table 1 Measured concentration (mean  $\pm$  1 standard deviation (SD)) of pollutants by district and land-use type (May 2021–December 2024)

| Pollutants                                 | Gasabo ( $n = 51\,534$ )  | Kicukiro ( $n = 21\,602$ ) | Nyarugenge ( $n = 34\,981$ )       | <sup>a</sup> $p$ value |
|--|---------------------------|----------------------------|------------------------------------|------------------------|
| PM <sub>2.5</sub> [ $\mu\text{g m}^{-3}$ ] | $37.9 \pm 17.5$           | $41.5 \pm 16.2$            | $45.8 \pm 27.6$                    | $<0.001$               |
| NO <sub>2</sub> [ $\mu\text{g m}^{-3}$ ]   | $21.2 \pm 6.5$            | $15.2 \pm 4.2$             | $22.9 \pm 6.5$                     | $<0.001$               |
| O <sub>3</sub> [ppb]                       | $18.9 \pm 6.6$            | $21.6 \pm 8.0$             | $25.5 \pm 18.4$                    | $<0.001$               |
| <b>Meteorological parameters</b>           |                           |                            |                                    |                        |
| Temperature ( $^\circ\text{C}$ )           | $20.8 \pm 4.1$            | $20.2 \pm 2.8$             | $20.7 \pm 4.3$                     | $<0.001$               |
| Relative humidity (%)                      | $62.6 \pm 14.0$           | $61.4 \pm 12.2$            | $62.6 \pm 13.9$                    | $<0.001$               |
| Pollutants                                 | Roadside ( $n = 7\,942$ ) | Rural ( $n = 72\,454$ )    | Urban background ( $n = 27\,721$ ) | <sup>a</sup> $p$ value |
| PM <sub>2.5</sub> [ $\mu\text{g m}^{-3}$ ] | $52.2 \pm 32.2$           | $37.5 \pm 17.1$            | $42.3 \pm 18.4$                    | $<0.001$               |
| NO <sub>2</sub> [ $\mu\text{g m}^{-3}$ ]   | $19.3 \pm 5.9$            | $21.4 \pm 6.8$             | $20.6 \pm 6.8$                     | $<0.001$               |
| O <sub>3</sub> [ppb]                       | $28.3 \pm 25.3$           | $21.1 \pm 7.1$             | $19.4 \pm 7.8$                     | $<0.001$               |
| <b>Meteorological parameters</b>           |                           |                            |                                    |                        |
| Temperature ( $^\circ\text{C}$ )           | $20.7 \pm 4.8$            | $20.2 \pm 3.7$             | $21.8 \pm 3.5$                     | $<0.001$               |
| Relative humidity (%)                      | $65.3 \pm 14.9$           | $63.1 \pm 13.2$            | $57.9 \pm 12.5$                    | $<0.001$               |

<sup>a</sup>  $p$ -value expresses the presence of statistically significant differences among the three districts and land-use types.



Panel A illustrates that  $PM_{2.5}$  levels exhibit a bimodal distribution, peaking in January and between June and September. Roadside sites consistently show the highest levels, roughly  $70 \mu\text{g m}^{-3}$ , while urban background zones are around  $55 \mu\text{g m}^{-3}$ , and rural areas are near  $50 \mu\text{g m}^{-3}$ . These trends indicate higher pollution during dry periods, probably driven by increased vehicle emissions, biomass burning, and dust resuspension.

$NO_2$  levels (Panel B) showed less seasonal variation, but consistently higher concentrations were observed at rural and urban background sites ( $\sim 22\text{--}23 \mu\text{g m}^{-3}$ ) than at roadside sites ( $\sim 20 \mu\text{g m}^{-3}$ ). This seemingly counterintuitive pattern may suggest contributions from diffuse sources, such as domestic burning, and from topographical features that encourage pollutant accumulation. Kigali's hilly terrain features valleys and basins where rural and background sites are often located. These low-lying areas experience airflow stagnation, leading to the accumulation of  $NO_2$  from domestic combustion and other diffuse sources. In contrast, roadside sites are often situated on steeper slopes and benefit from greater dispersion due to enhanced airflow, which helps explain the lower  $NO_2$  levels observed. This pattern may also reflect near-road chemistry, where freshly emitted traffic  $NO$  has not yet oxidized to  $NO_2$ , leading to lower measured  $NO_2$  at roadside sites despite higher total  $NO_x$  emissions. Ozone levels (Panel C) display clear seasonal variations across Kigali, reaching approximately 58 ppb at roadside sites in January. This significant increase corresponds to the dry season, and the elevated January mean  $O_3$  value was primarily driven by a pronounced surge in January 2022, particularly at the roadside sites. A Kigali-based study reported that January 2022 experienced the most intense and prolonged heatwave of the 2021–2024 period, with multiple consecutive days exceeding  $32 \text{ }^\circ\text{C}$ , during which ozone concentrations increased progressively.<sup>36</sup> Elevated temperatures are known to accelerate photochemical reactions, enhance atmospheric stagnation, and thereby amplify surface ozone formation.<sup>42,43</sup> However, ozone formation is also influenced by multiple meteorological and chemical factors, and the use of

low-cost electrochemical sensors may introduce additional uncertainty. Therefore, elevated  $O_3$  observed at the roadside (Fig. 3C) should be interpreted cautiously. Future studies incorporating co-located reference-grade  $O_3$  monitoring with RAMP  $O_3$  sensors and multivariate chemical analysis to confirm the contributions of photochemistry, titration dynamics, and meteorological variability are required.<sup>42,43</sup> After February, ozone levels drop sharply and stabilize around 20 ppb during the rainy season in mid-year and during the coldest month in Rwanda (March and April). This seasonal pattern reflects broader trends observed throughout sub-Saharan Africa. For instance, similar ozone peaks during the dry season were observed in semi-natural African areas such as wet savannas and humid forests, driven by biomass burning, photochemical reactions, and regional transport,<sup>44</sup> although Kigali's urban levels are higher. Kigali's roadside ozone levels approach those in Louis Trichardt, South Africa ( $\sim 30.8 \pm 8.0$  ppb), and suggest the consistent impact of meteorological and chemical conditions on regional ozone formation. The observed seasonal trends, particularly elevated  $PM_{2.5}$  and  $O_3$  concentrations during January and mid-year, coincide with Kigali's dry seasons, when reduced rainfall and humidity limit wet deposition, enabling greater pollutant accumulation. Increased solar radiation during these months enhances photochemical  $O_3$  formation, while dry soils and anthropogenic activity contribute to elevated  $PM_{2.5}$  through dust resuspension and combustion emissions. These patterns are consistent with findings from a previous study, which reported that  $PM_{2.5}$  concentrations in Kigali during the dry season were nearly double those in the wet season. This underscores the importance of integrating seasonal meteorology into air quality forecasting and pollution control strategies in Rwanda. Beyond seasonal forcing, the observed contrasts across land-use types likely reflect interactions between emission timing, atmospheric chemistry, and boundary-layer dynamics. During dry months, reduced wet deposition and enhanced vertical mixing can amplify  $PM_{2.5}$  and  $O_3$  accumulation, while delayed  $NO$ – $NO_2$  oxidation and terrain-driven stagnation may explain elevated background  $NO_2$  despite lower roadside values. These results underscore Kigali's heightened vulnerability to dry-season ozone pollution, with important consequences for public health and urban planning.

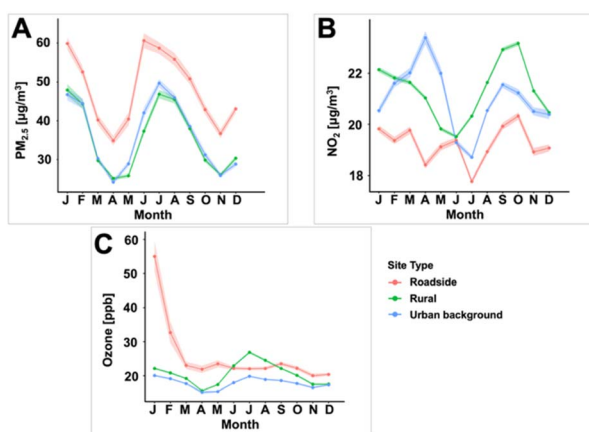


Fig. 3 Monthly average variations in concentrations of (A)  $PM_{2.5}$ , (B)  $NO_2$ , and (C)  $O_3$  across three site classifications: roadside, rural, and urban background. Shaded areas represent  $\pm 1$  standard error of the mean (SEM).

#### 3.4 Hourly patterns in mean $PM_{2.5}$ , $NO_2$ , and $O_3$ levels across site types

Fig. 4 illustrates the daily variations in mean  $PM_{2.5}$ ,  $NO_2$ , and  $O_3$  levels across different site types in Kigali.  $PM_{2.5}$  (Panel A) shows a clear bimodal pattern, with peaks early in the morning (06:00–08:00) and in the evening (18:00–21:00), particularly at roadside locations. This indicates that vehicular emissions play a major role during rush hours, aligning with results from similar urban research.<sup>45</sup> However, the sharp midday decline in  $PM_{2.5}$  between 09:00 and 17:00 likely reflects reduced traffic activity<sup>26</sup> combined with enhanced atmospheric dispersion driven by increased solar radiation, boundary-layer mixing, and wind speed.

Panel B shows  $NO_2$  with a dual-peak pattern, but its amplitude varies less across site types, indicating common combustion



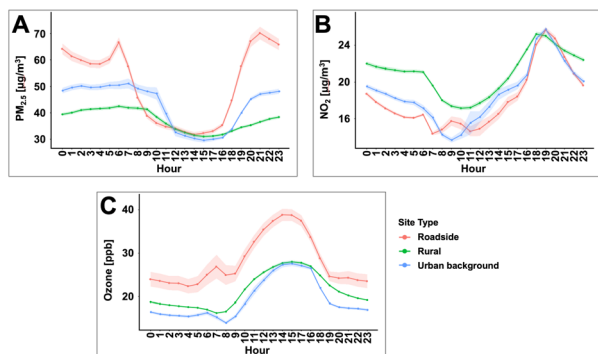


Fig. 4 Hourly (time is Rwanda local time, UTC + 2) variation in mean  $PM_{2.5}$  (Panel A),  $NO_2$  (Panel B), and ozone (Panel C) concentrations across roadside, rural, and urban background sites. Shaded areas represent  $\pm 1$  standard error of the mean (SEM).

emissions.<sup>45</sup> Notably, midday decreases in  $NO_2$  levels coincide with rises in  $O_3$  levels (Panel C), suggesting photochemical production of  $O_3$  from  $NO_2$ .  $O_3$  shows a sharp increase starting mid-morning, peaking between 14:00–17:00, especially at roadside sites, before declining after sunset. This pattern matches the dry-season photochemistry previously observed in sub-Saharan cities.<sup>44</sup> The sharper  $O_3$  peaks at roadside sites may reflect increased  $NO$  emissions from vehicles, which suppress early  $O_3$  levels *via* titration but amplify formation later as  $NO_2$  photolyzes. This reinforces the influence of traffic patterns on diurnal pollutant dynamics and underscores the nonlinear chemistry between primary and secondary pollutants. Overall, the data highlight the temporal link between traffic emissions and secondary pollutant formation, emphasizing the importance of time-specific mitigation strategies during peak exposure periods.

### 3.5 Temporal heterogeneity in air quality across four years in Kigali

Air quality trends over four years from 2021 to 2024 in Kigali reveal marked temporal heterogeneity in pollutant concentrations.  $PM_{2.5}$  concentrations exhibited statistically significant temporal variation over the four-year period ( $p < 0.001$ ). The annual mean concentration was highest in 2021 ( $45.5 \mu g m^{-3}$ ), decreased moderately in 2022 ( $42.3 \mu g m^{-3}$ ), dropped markedly in 2023 ( $35.0 \mu g m^{-3}$ ), and then rose again in 2024 ( $44.1 \mu g m^{-3}$ ), indicating a non-linear trend with a pronounced dip in 2023 (Fig. 5).  $NO_2$  concentrations also varied significantly over time ( $p < 0.001$ ), increasing from  $18.4 \mu g m^{-3}$  in 2021 to  $20.2 \mu g m^{-3}$  in 2022, slightly declining in 2023 ( $21.9 \mu g m^{-3}$ ), and peaking at  $23.4 \mu g m^{-3}$  in 2024. In contrast,  $O_3$  levels showed a downward trend from 26.3 ppb in 2021 to 19.2 ppb in 2023, followed by a modest increase in 2024 (21.6 ppb), with statistically significant differences across years ( $p < 0.001$ ).

Meteorological parameters also exhibited small but significant inter-annual variations. Mean temperature increased from  $20.3 \text{ }^\circ\text{C}$  in 2021 to  $21.2 \text{ }^\circ\text{C}$  in 2024, with a slight dip to  $20.2 \text{ }^\circ\text{C}$  in 2022. Relative humidity fluctuated more noticeably, reaching a peak of 64.4% in 2022 and a low of 60.5% in 2021 ( $p < 0.001$ ), highlighting the influence of climatic factors on pollutant

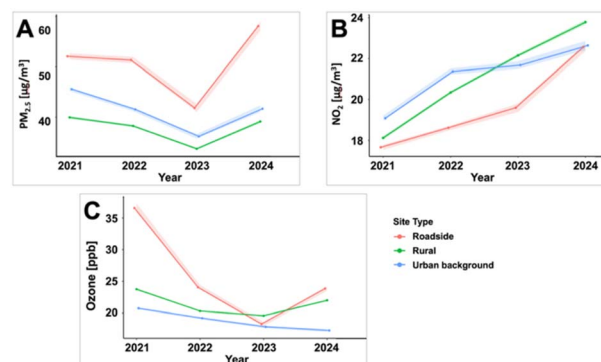


Fig. 5 Annual variation in mean  $PM_{2.5}$  (Panel A),  $NO_2$  (Panel B), and ozone (Panel C) concentrations across roadside, rural, and urban background sites from 2021 to 2024. Shaded areas represent  $\pm 1$  standard error of the mean (SEM).

dynamics. The annual dip in  $PM_{2.5}$  observed in 2023 appears consistent across districts and coincides with increased relative humidity and lower  $O_3$  levels, suggesting enhanced wet deposition and reduced photochemical activity. This aligns with findings from a recent study in Kigali,<sup>26</sup> which reported that elevated humidity in Kigali contributes to pollutant removal through washout processes. Conversely, the 2024 rebound aligns with drier conditions, reinforcing the role of meteorology in shaping interannual variations in air quality. While elevated temperatures enhance photochemical ozone production,<sup>46</sup> inter-annual variations in ambient  $O_3$  concentrations are not solely explained by temperature. Evidence suggests that factors such as relative humidity, rainfall, precursor availability, and atmospheric dynamics play substantial roles in modulating yearly ozone levels.<sup>47</sup> In 2023, the lower  $O_3$  levels may be explained by the heavy rainfall and flooding events that characterized the year.<sup>48</sup> In contrast,  $NO_2$  exhibited a more monotonic increase over time, consistent with changes in combustion-related emissions and urban activity rather than direct modulation by meteorological variability alone.

## 4 Discussion

This study presents a robust analysis of ambient air pollution in Kigali, focusing on  $PM_{2.5}$ ,  $NO_2$ , and  $O_3$  across spatial and temporal scales. The higher  $PM_{2.5}$  values observed in Nyarugenge highlight the influence of dense traffic and commercial activities in central urban areas. In contrast, Kicukiro and Gasabo, while showing lower levels, still far exceed the WHO's recommended annual mean of  $5 \mu g m^{-3}$  (WHO, 2021). These elevated levels reflect a citywide burden, consistent with earlier studies in Kigali,<sup>49</sup> and comparable to those in African urban centres such as Accra, Nairobi, and Lagos.<sup>50,51</sup> While  $PM_{2.5}$  concentrations in Kigali remain lower than those in megacities like Delhi, Cairo, Xi'an, and Beijing ( $>89.0 \mu g m^{-3}$ ), they are significantly higher than in cleaner cities such as Toronto, Paris, Amsterdam, and Helsinki ( $<10.0 \mu g m^{-3}$ ).<sup>52,53</sup>

Spatial analysis of  $NO_2$  shows Nyarugenge with the highest average concentrations, likely due to its status as the



commercial and transit hub. Gasabo's peak  $\text{NO}_2$  value suggests episodic spikes possibly linked to industrial or transport emissions. Kigali's average  $\text{NO}_2$  levels ( $20.8 \mu\text{g m}^{-3}$ ) exceed the WHO 2021 air quality guideline of  $10 \mu\text{g m}^{-3}$ , indicating sustained exposure above health-based recommendations. While these levels align with those observed in other African cities, such as Lagos ( $24 \mu\text{g m}^{-3}$ ),<sup>54</sup> they are lower than those in Asian cities like Seoul, Tokyo, and Beijing.<sup>55</sup> Compared to megacities in Europe, Kigali's urban background  $\text{NO}_2$  ( $20.6 \mu\text{g m}^{-3}$ ) exceeds those reported in the UK ( $13.1 \mu\text{g m}^{-3}$ ) and Paris ( $17 \mu\text{g m}^{-3}$ ) urban background sites, whereas roadside measurements ( $19.3 \mu\text{g m}^{-3}$ ) are comparable to those in the UK ( $20.7 \mu\text{g m}^{-3}$ ) but lower than those at traffic sites in Paris ( $40 \mu\text{g m}^{-3}$ ).<sup>56,57</sup> These patterns observed in Kigali suggest an increasing urban influence but also reflect early stages of motorization and industrial growth.

Ozone concentrations showed complex spatial behaviour. The high  $\text{O}_3$  in Nyarugenge may result from photochemical smog formation under urban heat conditions. Kigali's mean  $\text{O}_3$  values (22.1 ppb) remain below the WHO 2021 peak-season guideline of 30 ppb. However, dry-season 8 h maxima approach 58 ppb, indicating that episodic exceedances of health-based thresholds may occur during periods of enhanced photochemical activity. Kigali's mean  $\text{O}_3$  concentration (22.1 ppb) falls within the mid-range of global urban levels, generally lower than those reported in heavily polluted Asian megacities and comparable to many European and North American cities.<sup>58</sup> It is similar to the 2021 annual mean reported for Türkiye (22.6 ppb), though Türkiye's peak-season mean was higher (34.8 ppb).<sup>59</sup> Kigali's mean is, however, lower than the annual averaged daily maximum 8 hour  $\text{O}_3$  reported for Lisbon, Portugal, at both traffic (34.4 ppb) and non-traffic (39.1 ppb) sites.<sup>60</sup>

The study also observed clear pollutant gradients by site type. Roadside locations recorded the highest  $\text{PM}_{2.5}$  levels, consistent with patterns observed in Hong Kong, Sydney, and Dar es Salaam.<sup>61–63</sup> Rural  $\text{PM}_{2.5}$  levels, though lower, still exceeded WHO guidelines, underscoring the pervasive influence of biomass burning and pollutant transport. Similar rural trends have been reported in southwestern Uganda and the North China Plain.<sup>64,65</sup>

Microenvironmental differences were also evident in  $\text{NO}_2$  and  $\text{O}_3$  concentrations. While roadside  $\text{NO}_2$  levels were elevated, rural areas occasionally exceeded urban levels, indicating wider combustion activity. Urban background sites had slightly lower pollutant levels, influenced by diffuse emissions and spatial dispersion. These findings are consistent with global observations, which show that background and rural sites exhibit lower but persistent pollution burdens.<sup>66,67</sup>

Meteorological parameters contributed to observed pollutant behaviours. Warmer temperatures in Nyarugenge facilitated  $\text{O}_3$  formation, while relative humidity patterns influenced  $\text{PM}_{2.5}$  persistence. Kigali's thermal and humidity conditions paralleled patterns in Kampala and tropical African ecotones,<sup>68,69</sup> affirming the role of microclimate in air quality dynamics. These factors suggest that pollutant concentrations are not merely a result of emissions but are shaped by Kigali's meteorology and topography.

Finally, the diurnal and seasonal heterogeneity observed across the four years supports the objective of characterizing temporal variability. While  $\text{PM}_{2.5}$  showed seasonal peaks during dry months,  $\text{O}_3$  varied with temperature and precursor availability. The  $\text{NO}_2$  trend, with gradual increases over time, parallels urbanization and traffic growth, reinforcing the need for anticipatory urban planning. These findings build an evidence base for Kigali's air quality management, particularly in prioritizing roadside and high-density urban zones for intervention. They also underscore the potential of integrating air quality monitoring with climate-sensitive urban development policies.

## 5 Study limitations

While this study presents a comprehensive multi-year assessment of Kigali's ambient air quality, the spatial distribution of monitoring sites may not fully capture hyperlocal variations, especially within informal settlements or topographically complex areas. Second, although meteorological data were integrated to contextualize pollutant dynamics, localized weather phenomena such as inversion layers and microclimate effects were not fully modelled.

Third, although RAMP devices provide cost-effective and scalable monitoring solutions, they are susceptible to calibration drift over time, sensor aging, and cross-sensitivity to environmental conditions such as humidity and temperature. Despite validation efforts and periodic co-location with reference-grade monitors, discrepancies may still exist in the recorded pollutant concentrations. Fourth, without chemical speciation, which is beyond the scope of this work, it is not possible to apportion  $\text{PM}_{2.5}$  into dust, primary emissions, or secondary aerosol components, limiting the specificity of policy interventions. Lastly, although  $\text{O}_3$  levels were assessed, the lack of concurrent VOC and NO measurements precludes identification of the  $\text{O}_3$  formation regime ( $\text{NO}_x$ -vs. VOC-limited), which is critical for designing effective ozone mitigation strategies. These limitations, while common in low-resource settings, underscore the need for expanded monitoring infrastructure and modeling capacity in future work. Nevertheless, the study provides a strong foundation for evidence-based air quality policy and intervention design in Rwanda and similar settings.

## 6 Conclusions and implications

This study provides a comprehensive spatiotemporal assessment of  $\text{PM}_{2.5}$ ,  $\text{NO}_2$ , and  $\text{O}_3$  in Kigali, revealing consistently high pollutant levels across districts and site types. The findings demonstrate significant spatial variability, with Nyarugenge showing the highest concentrations of  $\text{PM}_{2.5}$  and  $\text{O}_3$ , and Gasabo peaking in  $\text{NO}_2$ . Roadside environments emerged as pollution hotspots, while even rural areas displayed concerning levels due to combustion sources and pollutant transport.

Temporally, pollutant levels fluctuated across the study period, with  $\text{PM}_{2.5}$  showing a temporary decline followed by a rebound, and  $\text{NO}_2$  reflecting a steady increase likely tied to urban growth.  $\text{O}_3$  exhibited nonlinear changes influenced by precursor levels and meteorological conditions. Kigali's air



quality indicators, although moderate in global comparison, exceed WHO guidelines and indicate increasing urban pressure on environmental health.

These findings emphasize the urgent need for targeted mitigation strategies in Kigali, including cleaner transportation, improved waste management, and strengthened monitoring systems. By aligning with national and regional policy frameworks, these actions can support sustainable urban development and reduce pollution-related health risks.

## 7 Policy considerations

To address the persistent air pollution challenges in Kigali and similar urban centres across sub-Saharan Africa, a multi-pronged policy response is necessary. First, governments must expand and institutionalize air quality monitoring networks. These systems should integrate reference-grade instruments with validated, low-cost sensors, complemented by meteorological data. Such networks will enhance the spatial and temporal resolution of pollution data, enabling robust early warning systems and evidence-based policy formulation. Second, establishing and enforcing national ambient air quality standards is critical. While the WHO provides global benchmarks, many African countries either lack national standards or do not enforce them effectively.<sup>70–72</sup> Governments should develop context-specific, legally binding thresholds informed by local emission patterns and health risk data, and ensure periodic revisions in line with emerging scientific evidence.

Targeted emission control strategies must also be scaled. Interventions in high-risk zones, such as urban cores, traffic corridors, and peri-urban communities, could include low-emission zones, improved public transit, bans on open burning, and incentives for clean household energy, especially in informal and rural settings where biomass use is widespread. Furthermore, regional cooperation should be strengthened. Air pollution transcends national borders, necessitating harmonized strategies among regional blocs such as the African Union (AU), the East African Community (EAC), the Economic Community of West African States (ECOWAS), and the Southern African Development Community (SADC). These bodies should promote joint action on transboundary pollutants, facilitate data sharing, and coordinate efforts on shared sources like biomass burning and dust transport.

Lastly, public engagement and transparency are essential. Open-access platforms for real-time air quality data and targeted risk communication campaigns can empower communities, support exposure reduction, and galvanize public advocacy. Collectively, these measures are critical to improving environmental governance and protecting population health.

## Author contributions

A. O. and E. K. contributed to conceptualization, methodology, investigation, and formal analysis. A. O. wrote the original draft, and D. T. contributed to editing. E. K. contributed to reviewing.

## Conflicts of interest

There are no conflicts to declare.

## Data availability

Data will be made available upon reasonable request from the corresponding author (Email: ekalisa2@uwo.ca).

## Acknowledgements

We acknowledge the air quality data provided by the Rwanda Environmental Management Authority. We also recognize the data obtained from the US Embassy in Rwanda's air monitoring station. EK acknowledges funding from the Natural Sciences and Engineering Research Council of Canada – Discovery grant (R7515A05).

## Notes and references

- 1 World Health Organization, Health impacts, <https://www.who.int/teams/environment-climate-change-and-health/air-quality-energy-and-health/health-impacts>, accessed 14 January 2026.
- 2 P. Sicard, E. Agathokleous, S. C. Anenberg, A. De Marco, E. Paoletti and V. Calatayud, *Sci. Total Environ.*, 2023, **858**, 160064, DOI: [10.1016/j.scitotenv.2022.160064](https://doi.org/10.1016/j.scitotenv.2022.160064).
- 3 World Health Organization, WHO global air quality guidelines, <https://www.who.int/publications/i/item/9789240034228>, accessed 19 January 2026.
- 4 Organization for Economic Cooperation and Development, The Economic Consequences of Outdoor Air Pollution, [https://www.oecd.org/en/publications/the-economic-consequences-of-outdoor-air-pollution\\_9789264257474-en.html](https://www.oecd.org/en/publications/the-economic-consequences-of-outdoor-air-pollution_9789264257474-en.html), accessed 29 June 2025.
- 5 Health Effects Institute, The State of Air Quality and Health Impacts in Africa | State of Global Air, <https://www.stateofglobalair.org/resources/report/state-air-quality-and-health-impacts-africa>, accessed 13 September 2025.
- 6 M. S. Hammer, A. Van Donkelaar, C. Li, A. Lyapustin, A. M. Sayer, N. C. Hsu, R. C. Levy, M. J. Garay, O. V. Kalashnikova, R. A. Kahn, M. Brauer, J. S. Apte, D. K. Henze, L. Zhang, Q. Zhang, B. Ford, J. R. Pierce and R. V. Martin, *Environ. Sci. Technol.*, 2020, **54**, 7879–7890, DOI: [10.1021/acs.est.0c01764](https://doi.org/10.1021/acs.est.0c01764).
- 7 A. Van Donkelaar, R. V. Martin, C. Li and R. T. Burnett, *Environ. Sci. Technol.*, 2019, **53**, 2595–2611, DOI: [10.1021/acs.est.8b06392](https://doi.org/10.1021/acs.est.8b06392).
- 8 S. Avnery, D. L. Mauzerall, J. Liu and L. W. Horowitz, *Atmos. Environ.*, 2011, **45**, 2297–2309, DOI: [10.1016/j.atmosenv.2011.01.002](https://doi.org/10.1016/j.atmosenv.2011.01.002).
- 9 L. Sager, *J. Environ. Econ. Manag.*, 2025, **130**, 103112, DOI: [10.1016/j.jeem.2024.103112](https://doi.org/10.1016/j.jeem.2024.103112).
- 10 A. Jonidi Jafari, E. Charkhloo and H. Pasalari, *J. Environ. Health Sci. Eng.*, 2021, **19**, 1911–1940, DOI: [10.1007/s40201-021-00744-4](https://doi.org/10.1007/s40201-021-00744-4).



- 11 European Environment Agency, Air quality status report, 2025, <https://www.eea.europa.eu/en/analysis/publications/air-quality-status-report-2025>, accessed 14 January 2026.
- 12 Copernicus Atmosphere Monitoring Service, 2014-2024: A decade of air quality improvements in Europe | Copernicus, <https://atmosphere.copernicus.eu/2014-2024-decade-air-quality-improvements-europe>, accessed 14 January 2026.
- 13 S. Tabahriti, London air quality improves after expansion of levy on polluting cars, says report, *Reuters*, 2025, <https://www.reuters.com/world/uk/london-air-quality-improves-after-expansion-levy-polluting-cars-says-report-2025-03-07/>.
- 14 S. M. Gaita, J. Boman, M. J. Gatari, J. B. C. Pettersson and S. Janhäll, *Atmospheric Chem. Phys.*, 2014, **14**, 9977–9991, DOI: [10.5194/acp-14-9977-2014](https://doi.org/10.5194/acp-14-9977-2014).
- 15 J. Wang, A. S. Alli, S. N. Clark, M. Ezzati, M. Brauer, A. F. Hughes, J. Nimo, J. B. Moses, S. Baah, R. Nathvani, V. D. S. Agyei-Mensah, J. Baumgartner, J. E. Bennett and R. E. Arku, *Environ. Res. Lett.*, 2024, **19**, 034036, DOI: [10.1088/1748-9326/ad2892](https://doi.org/10.1088/1748-9326/ad2892).
- 16 S. Imane, B. Oumaima, K. Kenza, I. Laila, E. M. Youssef, S. Zineb and E. J. Mohamed, *Curr. Environ. Health Rep.*, 2022, **9**, 276–298, DOI: [10.1007/s40572-022-00350-y](https://doi.org/10.1007/s40572-022-00350-y).
- 17 J. Bahino, M. Giordano, M. Beekmann, V. Yoboué, A. Ochou, C. Galy-Lacaux, C. Liousse, A. Hughes, J. Nimo, F. Lemmouchi, J. Cuesta, A. K. Amegah and R. Subramanian, *Environ. Sci. Atmospheres*, 2024, **4**, 468–487, DOI: [10.1039/D4EA00012A](https://doi.org/10.1039/D4EA00012A).
- 18 J.-F. Léon, A. B. Akpo, M. Bedou, J. Djossou, M. Bodjrenou, V. Yoboué and C. Liousse, *Atmospheric Chem. Phys.*, 2021, **21**, 1815–1834, DOI: [10.5194/acp-21-1815-2021](https://doi.org/10.5194/acp-21-1815-2021).
- 19 N. B. Ngamlana, W. Malherbe, G. Gericke and R. L. J. Coetzer, *Int. J. Environ. Health Res.*, 2025, **35**, 220–232, DOI: [10.1080/09603123.2024.2350600](https://doi.org/10.1080/09603123.2024.2350600).
- 20 S. Bililign, S. S. Brown, D. M. Westervelt, R. Kumar, W. Tang, F. Flocke, W. Vizuete, K. Ture, F. D. Pope, B. Demoz, A. Asa-Awuku, P. F. Levelt, E. Kalisa, G. Raheja, A. Ndyabakira and M. J. Gatari, *Bull. Am. Meteorol. Soc.*, 2024, **105**, E1584–E1602, DOI: [10.1175/BAMS-D-23-0098.1](https://doi.org/10.1175/BAMS-D-23-0098.1).
- 21 L. M. Atuyambe, R. E. Arku, N. Naidoo, T. Kapwata, K. P. Asante, G. Cissé, B. Simane, C. Y. Wright and K. Berhane, *Ann. Glob. Health*, 2024, **90**, 76, DOI: [10.5334/aogh.4527](https://doi.org/10.5334/aogh.4527).
- 22 R. Subramanian, *et al.*, *Clean Air J.*, 2020, **30**(2), 1–15, DOI: [10.17159/caj/2020/30/2.8023](https://doi.org/10.17159/caj/2020/30/2.8023).
- 23 J. Wang, A. S. Alli, S. Clark, A. Hughes, M. Ezzati, A. Beddows, J. Vallarino, J. Nimo, J. Bedford-Moses, S. Baah, G. Owusu, E. Agyemang, F. Kelly, B. Barratt, S. Beevers, S. Agyei-Mensah, J. Baumgartner, M. Brauer and R. E. Arku, *Sci. Total Environ.*, 2022, **803**, 149931, DOI: [10.1016/j.scitotenv.2021.149931](https://doi.org/10.1016/j.scitotenv.2021.149931).
- 24 T. Kabera, S. Bartington, C. Uwanyirigira, P. Abimana and F. Pope, *Int. J. Environ. Stud.*, 2020, **77**, 998–1011, DOI: [10.1080/00207233.2020.1732067](https://doi.org/10.1080/00207233.2020.1732067).
- 25 H. L. DeWitt, J. Gasore, M. Rupakheti, K. E. Potter, R. G. Prinn, J. D. D. Ndikubwimana, J. Nkusi and B. Safari, *Atmospheric Chem. Phys.*, 2019, **19**, 2063–2078, DOI: [10.5194/acp-19-2063-2019](https://doi.org/10.5194/acp-19-2063-2019).
- 26 E. Kalisa, A. Sudmant, R. Ruberambuga and J. Bower, *Cities Health*, 2025, 1–12, DOI: [10.1080/23748834.2025.2468017](https://doi.org/10.1080/23748834.2025.2468017).
- 27 V. N. Matthaios, D. Pope, P. Koutrakis, C. O. Olopade and C. M. North, *Glob. Chall.*, 2025, **9**, e00108, DOI: [10.1002/gch2.202500108](https://doi.org/10.1002/gch2.202500108).
- 28 R. Borge, S. Lange and R. Kehew, *Clean Air J.*, 2023, **33**(2), 1–22, DOI: [10.17159/caj/2023/33/2.15605](https://doi.org/10.17159/caj/2023/33/2.15605).
- 29 T. Holloway, D. Miller, S. Anenberg, M. Diao, B. Duncan, A. M. Fiore, D. K. Henze, J. Hess, P. L. Kinney, Y. Liu, J. L. Neu, S. M. O'Neill, M. T. Odman, R. B. Pierce, A. G. Russell, D. Tong, J. J. West and M. A. Zondlo, *Annu. Rev. Biomed. Data Sci.*, 2021, **4**, 417–447, DOI: [10.1146/annurev-biodatasci-110920-093120](https://doi.org/10.1146/annurev-biodatasci-110920-093120).
- 30 A. Abera, J. Friberg, C. Isaxon, M. Jerrett, E. Malmqvist, C. Sjöström, T. Taj and A. M. Vargas, *Annu. Rev. Public Health*, 2021, **42**, 193–210, DOI: [10.1146/annurev-publhealth-100119-113802](https://doi.org/10.1146/annurev-publhealth-100119-113802).
- 31 P. D. M. C. Katoto, L. Byamungu, A. S. Brand, J. Mokaya, H. Strijdom, N. Goswami, P. De Boever, T. S. Nawrot and B. Nemery, *Environ. Res.*, 2019, **173**, 174–188, DOI: [10.1016/j.envres.2019.03.029](https://doi.org/10.1016/j.envres.2019.03.029).
- 32 E. Coker and S. Kizito, *Int. J. Environ. Res. Public Health*, 2018, **15**, 427, DOI: [10.3390/ijerph15030427](https://doi.org/10.3390/ijerph15030427).
- 33 C. H. Fuller and A. K. Amegah, *Int. J. Environ. Res. Public Health*, 2022, **19**, 6359, DOI: [10.3390/ijerph19116359](https://doi.org/10.3390/ijerph19116359).
- 34 Green Climate Fund, FP245: Green City Kigali – A New Model for Urban Development in Rwanda, <https://www.greenclimate.fund/project/fp245>, accessed 20 January 2026.
- 35 J. M. V. Ntamwiza and N. Ishimwe, *Urban Plan. Transp. Res.*, 2025, **13**, 2478134, DOI: [10.1080/21650020.2025.2478134](https://doi.org/10.1080/21650020.2025.2478134).
- 36 E. Kalisa and A. Sudmant, *Sci. Rep.*, 2025, **15**, 26448, DOI: [10.1038/s41598-025-12210-4](https://doi.org/10.1038/s41598-025-12210-4).
- 37 S. Gulia, S. M. Shiva Nagendra, M. Khare and I. Khanna, *Atmospheric Pollut. Res.*, 2015, **6**, 286–304, DOI: [10.5094/APR.2015.033](https://doi.org/10.5094/APR.2015.033).
- 38 The World Bank, World Bank Open Data, <https://data.worldbank.org>, accessed 10 October 2025.
- 39 C. Malings, R. Tanzer, A. Haurlyiuk, S. P. N. Kumar, N. Zimmerman, L. B. Kara, A. A. Presto and R. Subramanian, *Atmospheric Meas. Tech.*, 2019, **12**, 903–920, DOI: [10.5194/amt-12-903-2019](https://doi.org/10.5194/amt-12-903-2019).
- 40 N. Zimmerman, A. A. Presto, S. P. N. Kumar, J. Gu, A. Haurlyiuk, E. S. Robinson, A. L. Robinson and R. Subramanian, *Atmospheric Meas. Tech.*, 2018, **11**, 291–313, DOI: [10.5194/amt-11-291-2018](https://doi.org/10.5194/amt-11-291-2018).
- 41 H. L. DeWitt, J. Gasore, M. Rupakheti, K. E. Potter, R. G. Prinn, J. D. D. Ndikubwimana, J. Nkusi and B. Safari, *Atmospheric Chem. Phys.*, 2019, **19**, 2063–2078, DOI: [10.5194/acp-19-2063-2019](https://doi.org/10.5194/acp-19-2063-2019).
- 42 D. J. Jacob and D. A. Winner, *Atmos. Environ.*, 2009, **43**, 51–63, DOI: [10.1016/j.atmosenv.2008.09.051](https://doi.org/10.1016/j.atmosenv.2008.09.051).
- 43 A. M. Fiore, V. Naik, D. V. Spracklen, A. Steiner, N. Unger, M. Prather, D. Bergmann, P. J. Cameron-Smith, I. Cionni, W. J. Collins, S. Dalsøren, V. Eyring, G. A. Folberth,



- P. Ginoux, L. W. Horowitz, B. Josse, J.-F. Lamarque, I. A. MacKenzie, T. Nagashima, F. M. O'Connor, M. Righi, S. T. Rumbold, D. T. Shindell, R. B. Skeie, K. Sudo, S. Szopa, T. Takemura and G. Zeng, *Chem. Soc. Rev.*, 2012, **41**, 6663, DOI: [10.1039/C2CS35095E](https://doi.org/10.1039/C2CS35095E).
- 44 H. E. V. Donnou, A. B. Akpo, M. Ossouhou, C. Delon, V. Yoboué, D. Laouali, M. Ouafou-Leumbe, P. G. Van Zyl, O. Ndiaye, E. Gardrat, M. Dias-Alves and C. Galy-Lacaux, *Atmospheric Chem. Phys.*, 2024, **24**, 13151–13182, DOI: [10.5194/acp-24-13151-2024](https://doi.org/10.5194/acp-24-13151-2024).
- 45 R. Cichowicz and A. Steleǳowski, *Arch. Environ. Contam. Toxicol.*, 2019, **77**, 197–213, DOI: [10.1007/s00244-019-00627-8](https://doi.org/10.1007/s00244-019-00627-8).
- 46 U.S. Environmental Protection Agency, Trends in Ozone Adjusted for Weather Conditions, <https://www.epa.gov/air-trends/trends-ozone-adjusted-weather-conditions>, accessed 27 January 2026.
- 47 B. Chen, L. Zhen, L. Wang, H. Zhong, C. Lin, L. Yang, W. Xu and R.-J. Huang, *Sci. Total Environ.*, 2024, **953**, 176062, DOI: [10.1016/j.scitotenv.2024.176062](https://doi.org/10.1016/j.scitotenv.2024.176062).
- 48 Reuters, Rwanda floods kill 130, destroy over 5,000 houses, <https://www.reuters.com/business/environment/rwanda-floods-kill-130-destroy-over-5000-houses-2023-05-04/>, accessed 27 January 2026.
- 49 E. Kalisa, E. G. Nagato, E. Bizuru, K. C. Lee, N. Tang, S. B. Pointing, K. Hayakawa, S. D. J. Archer and D. C. Lacap-Bugler, *Environ. Sci. Technol.*, 2018, **52**, 12179–12187, DOI: [10.1021/acs.est.8b03219](https://doi.org/10.1021/acs.est.8b03219).
- 50 P. Gahungu, J. R. Kubwimana, L. J. M. B. Muhimpundu and E. Ndamuzi, *arXiv*, 2022, DOI: [10.48550/ARXIV.2208.12719](https://doi.org/10.48550/ARXIV.2208.12719), preprint.
- 51 S. D. X. Chua, O. Oguge, C. A. Oliewo, R. Sserunjogi, D. Okure, P. Adong, A. Manyele, T. Hussein, Y. Yang, X. Lu, K. Lehtipalo, M. A. Zaidan and T. Petäjä, *Environ. Sci. Technol. Lett.*, 2025, **12**, 1169–1176, DOI: [10.1021/acs.estlett.5c00451](https://doi.org/10.1021/acs.estlett.5c00451).
- 52 Z. Cheng, L. Luo, S. Wang, Y. Wang, S. Sharma, H. Shimadera, X. Wang, M. Bressi, R. M. De Miranda, J. Jiang, W. Zhou, O. Fajardo, N. Yan and J. Hao, *Environ. Int.*, 2016, **89–90**, 212–221, DOI: [10.1016/j.envint.2016.02.003](https://doi.org/10.1016/j.envint.2016.02.003).
- 53 M. W. Tessum, S. C. Anenberg, Z. A. Chafe, D. K. Henze, G. Kleiman, I. Kheirbek, J. D. Marshall and C. W. Tessum, *Atmos. Environ.*, 2022, **286**, 119234, DOI: [10.1016/j.atmosenv.2022.119234](https://doi.org/10.1016/j.atmosenv.2022.119234).
- 54 F. O. Abulude, U. Damodharan, S. Acha, A. Adamu and K. M. Arifalo, *Aerosol Sci. Eng.*, 2021, **5**, 275–284, DOI: [10.1007/s41810-021-00099-1](https://doi.org/10.1007/s41810-021-00099-1).
- 55 Y. Li, Y. Tang, Z. Fan, H. Zhou and Z. Yang, *Environ. Eng. Res.*, 2017, **23**, 21–27, DOI: [10.4491/eer.2017.006](https://doi.org/10.4491/eer.2017.006).
- 56 Department for Environment, Food & Rural Affairs (DEFRA), Nitrogen dioxide (NO<sub>2</sub>), <https://www.gov.uk/government/statistics/air-quality-statistics/nitrogen-dioxide>, accessed 24 February 2026.
- 57 V. Bougault, R. Valorso, R. Sarda-Esteve, D. Baisnee, N. Visez, G. Oliver, J. Bureau, F. Abdoussi, V. Gherzi and G. Foret, *Br. J. Sports Med.*, 2024, **58**, 973–982, DOI: [10.1136/bjsports-2024-108129](https://doi.org/10.1136/bjsports-2024-108129).
- 58 J. Ni, J. Jin, Y. Wang, B. Li, Q. Wu, Y. Chen, S. Du, Y. Li and C. He, *Geogr. Sustain.*, 2024, **5**, 64–76, DOI: [10.1016/j.geosus.2023.09.008](https://doi.org/10.1016/j.geosus.2023.09.008).
- 59 Ö. Zeydan and U. Ülker, *Environ. Monit. Assess.*, 2024, **196**, 549, DOI: [10.1007/s10661-024-12718-8](https://doi.org/10.1007/s10661-024-12718-8).
- 60 A. R. Soares, R. Deus, C. Barroso and C. Silva, *Atmosphere*, 2021, **12**, 183, DOI: [10.3390/atmos12020183](https://doi.org/10.3390/atmos12020183).
- 61 R. M. Njee, K. Meliefste, H. M. Malebo and G. Hoek, *J. Environ. Pollut. Hum. Health*, 2016, **4**(4), 83–90, DOI: [10.12691/jephh-4-4-2](https://doi.org/10.12691/jephh-4-4-2).
- 62 I. Wadlow, C. Paton-Walsh, H. Forehead, P. Perez, M. Amirghasemi, É.-A. Guérette, O. Gendek and P. Kumar, *Atmosphere*, 2019, **10**, 217, DOI: [10.3390/atmos10040217](https://doi.org/10.3390/atmos10040217).
- 63 K. L. So, H. Guo and Y. S. Li, *Atmos. Environ.*, 2007, **41**, 9427–9434, DOI: [10.1016/j.atmosenv.2007.08.053](https://doi.org/10.1016/j.atmosenv.2007.08.053).
- 64 D. Chen, X. Liu, J. Lang, Y. Zhou, L. Wei, X. Wang and X. Guo, *Sci. Total Environ.*, 2017, **583**, 280–291, DOI: [10.1016/j.scitotenv.2017.01.066](https://doi.org/10.1016/j.scitotenv.2017.01.066).
- 65 K. Desai, C. Mandell, J. Tumwesigire, C. Kayongo, E. Passell, S. Sagar, S. Onyango, S. Okello, M. Siedner, J. R. Balmes, S. Asimwe and C. M. North, *Am. J. Respir. Crit. Care Med.*, 2025, **211**, A2112, DOI: [10.1164/ajrccm.2025.211.Abstracts.A2112](https://doi.org/10.1164/ajrccm.2025.211.Abstracts.A2112).
- 66 N. Cheng, Y. Li, F. Sun, C. Chen, B. Wang, Q. Li, P. Wei and B. Cheng, *Aerosol Air Qual. Res.*, 2018, **18**, 343–356, DOI: [10.4209/aaqr.2017.02.0092](https://doi.org/10.4209/aaqr.2017.02.0092).
- 67 C. S. Malley, E. Von Schneidmesser, S. Moller, C. F. Braban, W. K. Hicks and M. R. Heal, *Atmospheric Chem. Phys.*, 2018, **18**, 3563–3587, DOI: [10.5194/acp-18-3563-2018](https://doi.org/10.5194/acp-18-3563-2018).
- 68 P. Kabano, A. Harris and S. Lindley, *Int. J. Biometeorol.*, 2022, **66**, 385–396, DOI: [10.1007/s00484-020-02061-1](https://doi.org/10.1007/s00484-020-02061-1).
- 69 I. K. Nooni, F. K. Ogou, A. A. Saidou Chaibou, S. K. Fianko, T. Atta-Darkwa and N. A. Prempeh, *Atmosphere*, 2025, **16**, 828, DOI: [10.3390/atmos16070828](https://doi.org/10.3390/atmos16070828).
- 70 Think Global Health, Tackling Air Pollution in Africa With Data, <https://www.thinkglobalhealth.org/article/tackling-air-pollution-africa-data>, accessed 20 January 2026.
- 71 E. Kalisa, M. L. Clark, T. Ntakirutimana, M. Amani and J. Volckens, *Heliyon*, 2023, **9**, e18450, DOI: [10.1016/j.heliyon.2023.e18450](https://doi.org/10.1016/j.heliyon.2023.e18450).
- 72 Health Effects Institute, The State of Air Quality and Health Impacts in Africa, State of Global Air, <https://www.stateofglobalair.org/resources/report/state-air-quality-and-health-impacts-africa#https://www.stateofglobalair.org/sites/default/files/documents/2022-10/the-state-of-air-quality-and-health-impacts-in-africa-press-release.pdf>, accessed 20 January 2026.

